

Scaling of Rayleigh-Taylor mixing in porous media

G. Boffetta , M. Borgnino, and S. Musacchio

Dipartimento di Fisica and INFN, Università di Torino, via P. Giuria 1, 10125 Torino, Italy



(Received 7 January 2020; accepted 4 June 2020; published 22 June 2020)

Pushing two fluids with different density one against the other causes the development of the Rayleigh-Taylor instability at their interface, which further evolves in a complex mixing layer. In porous media, this process is influenced by the viscous resistance experienced while flowing through the pores, which is described by the Darcy's law. Here, we investigate the mixing properties of the Darcy-Rayleigh-Taylor system in the limit of large Péclet number by means of direct numerical simulations in three and two dimensions. In the mixing zone, the balance between gravity and viscous forces results in a non-self-similar growth of elongated plumes, whose length increases linearly in time while their width follows a diffusive growth. The mass-transfer Nusselt number is found to increase linearly with the Darcy-Rayleigh number supporting a universal scaling in porous convection at high Ra numbers. Finally, we find that the mixing process displays important quantitative differences between two and three dimensions.

DOI: [10.1103/PhysRevFluids.5.062501](https://doi.org/10.1103/PhysRevFluids.5.062501)

Rayleigh-Taylor (RT) mixing is produced by a well-known instability at the interface of two fluids with different density in the presence of a relative acceleration. The instability develops in a nonlinear phase with a mixing layer which grows in time. Usually, RT mixing is studied for bulk fluids at low viscosity where the turbulent mixing layer grows as t^2 and produces velocity and temperature fluctuations which follow the Kolmogorov-Obukhov phenomenology in three dimensions (3D) [1] and the Bolgiano-Obukhov phenomenology in two dimensions (2D) [2–4]. RT turbulence has been extensively studied within the general framework of turbulent convection, and is today one of the prototypes of buoyancy-driven flow with a wide range of applications [5–7].

RT instability has also been studied in porous media, starting from the classical works on linear stability analysis [8] and the comparison with experiments in quasi-two-dimensional (quasi-2D) Hele-Shaw cells [9]. Recently, RT mixing in porous media has received renewed attention in view of its applications, in particular in CO₂ sequestration in saline aquifers. Dissolution of carbon dioxide in the aqueous phase increases its density and induces a buoyancy-driven instability which accelerates the process of CO₂ sequestration into the bulk of the aquifer [10–12]. Motivated by this application, several experimental and numerical studies of RT mixing have been reported, mostly in two dimensions [13,14], while few experiments in three dimensions have been performed [15].

In spite of their importance for applications, buoyancy-driven flows in porous media are much less known than their turbulent analog in bulk flow. RT mixing is not an exception and indeed its basic statistical properties are still not fully understood. In this Rapid Communication we study porous RT mixing by means of extensive three-dimensional direct numerical simulations (DNS) of Darcy's equation at different resolutions and diffusivities in order to achieve a possible asymptotic regime. By comparing the results of 3D and 2D numerical simulations at the same Péclet number we find similar qualitative behavior but significant quantitative differences. We find that in 3D the extension of the mixing layer grows linearly in time, in agreement with dimensional predictions and experimental findings [9] and in contrast with what has been observed recently in two dimensions where anomalous scaling has been reported [14]. The horizontal characteristic scale of plumes is

found to follow a diffusive law and therefore the mixing layer does not evolve in a self-similar way. We also find that the dimensionless mass flux, quantified by the Nusselt number, grows proportionally to the Darcy-Rayleigh number of the flow both in two and three dimensions, a result which confirms recent findings in Rayleigh-Bénard (RB) convection in porous media [16,17]. Surprisingly we find that, at a given Rayleigh number, the Nusselt number is larger in 2D than in 3D, while the opposite is observed for RB convection [17].

We consider the Darcy's equation for a single-phase (miscible) flow in an isotropic porous medium [18] in the Boussinesq approximation [19]

$$\mathbf{u} = \frac{\kappa}{\mu\phi}(-\nabla p + \rho\mathbf{g}), \quad (1)$$

$$\partial_t \rho + \mathbf{u} \cdot \nabla \rho = D \nabla^2 \rho, \quad (2)$$

where \mathbf{u} represents the velocity field (incompressible, i.e., $\nabla \cdot \mathbf{u} = 0$) and ρ is the density field. In (1) κ is the isotropic permeability, ϕ is the porosity, μ is the viscosity (which is assumed constant), D is the diffusivity coefficient, and $\mathbf{g} = (0, 0, -g)$ is the gravity acceleration. More generally, the flow $\mathbf{q} = \phi\mathbf{u}$ through a nonisotropic porous medium can be expressed in terms of the permeability tensor K_{ij} as $q_i = -K_{ij}(\partial_j p + \rho g \delta_{j3})/\mu$. Here we consider for simplicity the isotropic case $K_{ij} = \kappa \delta_{ij}$.

The Rayleigh-Taylor setup is obtained by taking an initial unstable step density profile with $\rho = \rho_0 - \Delta\rho/2$ for $-H/2 \leq z \leq 0$ and $\rho = \rho_0 + \Delta\rho/2$ for $0 \leq z \leq H/2$, where $\Delta\rho$ is the density jump. H and L are the vertical and horizontal sizes of the box, respectively. Given that the term $\rho_0\mathbf{g}$ in Eq. (1) can be absorbed in the hydrostatic pressure, in the numerical simulations we set $\rho_0 = 0$ without loss of generality. The only parameter which controls the dynamics of the system is the Péclet number $Pe = Lw_0/D$, where $w_0 = \frac{\kappa g}{\mu\phi} \Delta\rho$ is a characteristic velocity.

We perform extensive numerical simulations of the Darcy-Boussinesq equations (1) and (2) by means of pseudospectral code [20] in both two and three dimensions. The box sizes are $L = 2\pi$ and $H = 4L$ with a uniform numerical grid at resolution $M \times M \times 4M$. The boundary conditions are periodic in all the directions and we impose a zero-velocity mask around $z = \pm H/2$ (where the density stratification is stable). Time evolution is obtained by a second-order Runge-Kutta scheme with explicit linear part and the code is fully parallelized in one direction by using MPI libraries. The time step is chosen to satisfy the Courant criterion. In order to trigger the instability, a random perturbation is added in a narrow region around the interface at $z = 0$. Being interested in investigating the possible asymptotic regime and the effects of finite Pe on the growth law of the mixing layer, the values of Pe considered in our study are the highest permitted by the resolution of the simulation and are comparable with values reported for CO_2 sequestration [21].

Three flows at different diffusivities $D = 4 \times 10^{-4}$, $D = 2 \times 10^{-4}$, and $D = 10^{-4}$ (at resolutions $M = 512$, $M = 1024$, and $M = 2048$, respectively) are simulated, corresponding to Péclet numbers $Pe = 0.8 \times 10^4$, $Pe = 1.6 \times 10^4$, and $Pe = 3.1 \times 10^4$. In all cases the values of the diffusivity are sufficiently large to resolve the initial instability predicted by linear stability analysis, i.e., the maximum resolved wave number $k_{\max} = M/3$ is larger than $k^* = \frac{\sqrt{5}-2}{2D} w_0$ [22,23] ($k_{\max}/k^* = 1.16$). During the evolution of the mixing layer, the most energetic modes move to larger scales making this requirement less stringent [24,25]. The results are averaged over an ensemble of 2 simulations for the 3D case and 20 simulations for the 2D case with different initial random perturbations. Numerical results are made dimensionless by using L and $\tau = L/w_0$ as length and time units, respectively.

We first focus on the results of the 3D simulations. In Fig. 1 we show two snapshots of the density field at different times in the evolution of the mixing layer. One observes that heavy (light) plumes penetrating into light (heavy) domains become bigger and more elongated, suggesting the lack of self-similarity. In spite of the complexity of the mixing layer, the mean density vertical profile, defined as the average over horizontal planes $\bar{\rho}(z, t) = \langle \rho(\mathbf{x}, t) \rangle_{xy} = \frac{1}{L^2} \int \rho(\mathbf{x}, t) dx dy$, displays a self-similar evolution with a close-to-linear gradient in the central part, as shown in Fig. 2(a). The upper inset in Fig. 2(a) shows the density standard deviation $\sigma(z, t) \equiv \sqrt{\overline{\rho(z, t)^2} - \overline{\rho(z, t)}^2}$ inside

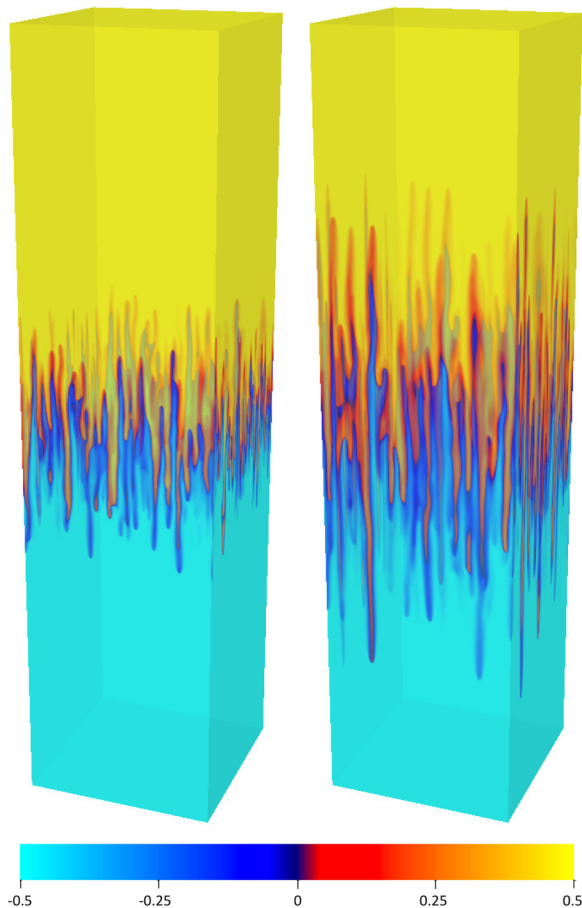


FIG. 1. Two snapshots of the density fields for the 3D simulation at $Pe = 1.6 \times 10^4$ at times $t = 2\tau$ (left) and $t = 4\tau$ (right). Colors represent the relative density.

the mixing layer at three different times. While the region of nonzero $\sigma(z)$ extends in time following the mixing layer, the peak value of σ remains approximately constant, indicating a lack of complete homogenization. We note that, in agreement with the Darcy's law (1), the profile of density standard deviation is equal to the profile of the rms vertical velocity, i.e., $\overline{w}_{\text{rms}}(z, t) = w_0 \sigma(z, t) / \Delta\rho$ [see lower inset of Fig. 2(a)].

The observed simple density profile allows a precise determination of the size of the mixing layer (i.e., regions in which density is not uniform and velocity is nonzero) by using a nonlinear diffusive model developed recently for turbulent RT mixing at high Reynolds numbers [26]. The model is based on an eddy diffusivity which depends on the local density and predicts for the mixing layer the polynomial profile $\rho(z) = \frac{\Delta\rho}{4} \frac{z}{z_1} [3 - (\frac{z}{z_1})^2]$ for $|z| \leq z_1$, where z_1 represents half size of the mixing layer. We find that the above cubic expression fits very well the density profiles shown in Fig. 2(a) and allows one to measure precisely the extension of the mixing layer as $h(t) = 2z_1(t)$. We remark that other definitions of the width of the mixing layer have been used, based on local threshold value [27] or global quantities [28]. When applied to our data these methods give results similar to the polynomial fit but with larger uncertainties.

The evolution of the mixing layer is shown in Fig. 2(b) for the 3D simulations at different diffusivities. We notice that, at variance with the turbulent case where it follows an accelerated law [6], here the mixing layer grows linearly in time as $h(t) = \alpha w_0 t$ where α is a dimensionless

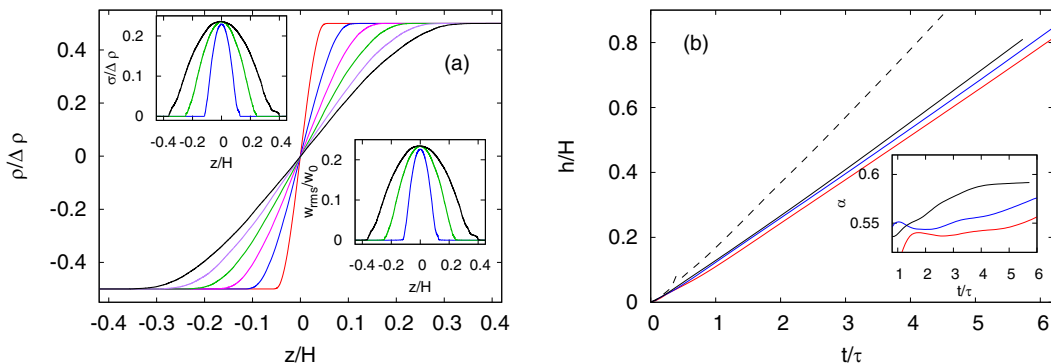


FIG. 2. Panel (a): Mean density profiles $\bar{\rho}(z, t)$ at times $t = 0.8\tau$ (red), $t = 1.6\tau$ (blue), $t = 2.4\tau$ (magenta), $t = 3.2\tau$ (green), $t = 4.0\tau$ (violet), and $t = 4.8\tau$ (black). Upper inset: density standard deviation $\sigma(z, t) = (\overline{\rho^2} - \bar{\rho}^2)^{1/2}$ at times $t = 1.6\tau$ (blue), $t = 3.2\tau$ (green), and $t = 4.8\tau$ (black). Lower inset: rms vertical velocity profile $\bar{w}_{\text{rms}}(z, t)$ at times $t = 1.6\tau$ (blue), $t = 3.2\tau$ (green), and $t = 4.8\tau$ (black). Simulation in 3D at $\text{Pe} = 3.1 \times 10^4$. Panel (b): Time evolution of the width of the mixing layer $h(t) = 2z_1(t)$ for the simulations at $\text{Pe} = 0.8 \times 10^4$ (red), $\text{Pe} = 1.6 \times 10^4$ (blue), and $\text{Pe} = 3.1 \times 10^4$ (black). The black dashed line represents the two-dimensional case with $\text{Pe} = 3.1 \times 10^4$. Inset: Time derivative dh/dt normalized with w_0 to give the value of the coefficient $\alpha = (dh/dt)/w_0 \simeq 0.59$.

coefficient which measures the efficiency of the process. The physical reason for the linear growth is that in porous media viscosity suppresses the inertial accelerating term and the velocity in the mixing layer reaches a constant value, which is proportional to the dimensional estimate w_0 . From the time derivative of $h(t)$ which, for the simulations at highest Pe, reaches a constant value at final times [see the inset of Fig. 2(b)] we are able to measure the value of the dimensionless coefficient $\alpha = (dh/dt)/w_0 \simeq 0.59$ with still a possible weak dependence on Pe.

From the point of view of dimensional analysis, the time derivative $\alpha = dh/dt$ and the peak value of the profile of w_{rms} can be considered equivalent quantities. Nonetheless, the convergence to the asymptotic regime for these two quantities may be different, because α depends on the global evolution of the mixing layer, while the peak of w_{rms} is attained in a narrow central region. In particular, our results indicate that the saturation of the peak value of w_{rms} anticipates the constant- α regime. Indeed, by comparing the insets of Figs. 2(a) and 2(b), we observe that in the simulation with the largest Pe at time $t \sim 1.6\tau$ the peak value of the profile of w_{rms} has already become constant, while α has not yet reached a constant plateau. Moreover, we have found that the peak of the profile of w_{rms} reaches a constant value also in the 3D simulations at lower Pe in which the regime of constant α is not yet attained.

The extension of the mixing layer defines the (time-dependent) Darcy-Rayleigh number of the flow measuring the ratio of diffusive to buoyancy timescales and defined here as $\text{Ra} = \frac{w_0 h}{D}$. At large values of Ra density fluctuations are transported by buoyancy forces and the efficiency of this process is quantified by the mass-transfer Nusselt number $\text{Nu} = \frac{\langle w\rho\rangle h}{D\Delta\rho}$ (brackets indicate average over the physical domain). The classical argument for the dependence of Nu over Ra assumes that, at large values of Ra the density flux becomes independent on h and, for a porous medium, predicts an “ultimate” linear scaling $\text{Nu} \simeq \text{Ra}$. The linear scaling is also a rigorous bound for Rayleigh-Bénard porous convection [29,30] and has been observed in numerical simulations of porous Rayleigh-Bénard convection both in 2D [16] and in 3D [17].

Figure 3(a) shows the dependence of Nu over Ra for the 3D runs at higher resolutions. For large values of Ra a linear regime is evident (and confirmed by the derivative shown in the inset) for which $\text{Nu} \simeq 0.031\text{Ra}$. This ultimate regime can be predicted for the case of RT mixing from the definition of Nu by assuming a constant $\langle w\rho\rangle = c w_0 \Delta\rho$ which gives $\text{Nu} = c\text{Ra}$. The coefficient $c \simeq 0.031$

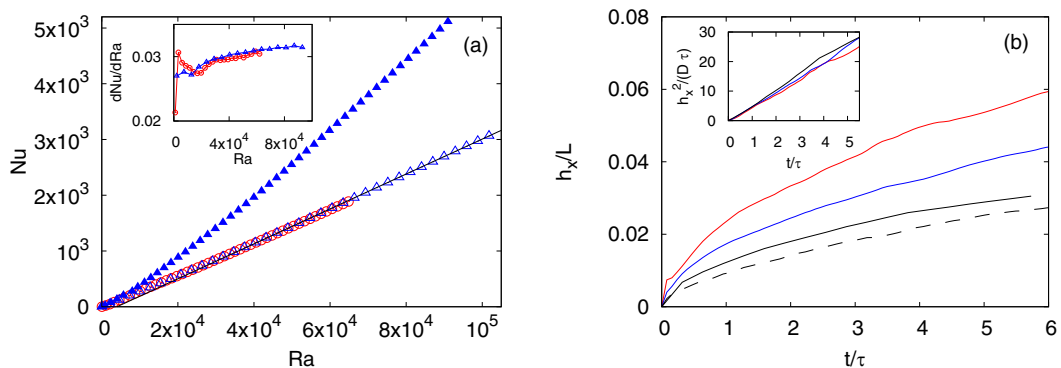


FIG. 3. Panel (a): Nusselt number as a function of the Rayleigh number for the simulations at $Pe = 1.6 \times 10^4$ (red open circles) and $Pe = 3.1 \times 10^4$ (blue open triangles). Blue filled triangles represent the results for the 2D case ($Pe = 3.1 \times 10^4$). The black line represents the linear dependence $Nu = 0.031Ra - 124.9$. Inset: derivative $d(Nu)/d(Ra)$ for the two three-dimensional cases (symbols as above). Panel (b): Time evolution of the horizontal correlation scale $h_x(t)$ for the simulations at $Pe = 0.8 \times 10^4$ (red), $Pe = 1.6 \times 10^4$ (blue), and $Pe = 3.1 \times 10^4$ (black). The black dashed line represents the results for the two-dimensional case with $Pe = 3.1 \times 10^4$. Inset: Square horizontal scale h_x^2 rescaled with $D\tau$ demonstrating diffusive growth.

measures the strength of the correlations between density fluctuations and vertical velocity induced by the Darcy law.

From Fig. 1 it is evident that density plumes become wider while elongating in the mixing layer. To quantify this process we compute the characteristic horizontal scale of plumes h_x defined as the first zero crossing of the horizontal autocorrelation function of density $c(r, t) = \langle \rho(x + r, y, 0, t) \rho(x, y, 0, t) \rangle_{xy} / \langle \rho(x, y, 0, t) \rangle_{xy}^2$, computed on the middle plane $z = 0$. Figure 3(b) shows the time evolution of $h_x(t)$ for the three different simulations with different Pe . We notice that here lines are in the opposite order with respect to Fig. 2(b), i.e., h_x grows faster for the larger diffusivity. Indeed, as shown in the inset of Fig. 3(b), the evolution of horizontal scale is compatible with a diffusive growth $h_x(t)^2 \propto Dt$. Nonetheless we remark that the diffusive growth of h_x is the result of nonlinear processes including plume merging and coarsening and it is not a simple direct consequence of molecular diffusion.

The observation of a linear growth of the vertical scale [Fig. 2(b)] and the diffusive increase of the horizontal scale [Fig. 3(b)] indicates that two different processes are active in the dynamics of the mixing layer and that its evolution is not self-similar, at variance with the turbulent case. The ballistic (diffusive) evolution of the vertical (horizontal) scales has also been observed in quasi-2D Hele-Shaw cells and in 2D simulations [9,13] (with possible anomalous corrections for the vertical motion [14]) and this suggests a possible universality of porous RT mixing with respect to dimensionality. It is therefore interesting to directly compare our 3D results with corresponding 2D cases. To this aim, we have performed a set of numerical simulations for the two-dimensional version of (1) with the same resolutions and diffusivities. The results in this case have been averaged over ten independent realizations.

In Fig. 2(b) we plot the evolution of the mixing layer for the two-dimensional simulations at the highest resolution and Péclet ($Pe = 3.1 \times 10^4$). After an initial regime in which the growth of $h(t)$ is faster than ballistic, at large times a linear growth is observed also in 2D but with a coefficient α which is about 40% larger than in the 3D case ($\alpha_{2D} \simeq 0.84$). The faster growth of the mixing layer in two dimensions is a consequence of density plumes which are more elongated and thinner than in the 3D case. This is confirmed by Fig. 3(b), which shows that the horizontal correlation scale in the 2D case is smaller than in the 3D counterpart.

For the 2D simulations at lower Pe ($Pe = 0.8 \times 10^4$ and $Pe = 1.6 \times 10^4$, not shown here) no linear regime is reached before h reaches the size of the box and a faster-than-ballistic growth is observed, in agreement with recent studies [14]. Although the main goal of our work is not the precise measurement of the scaling exponent $h(t) \sim t^\gamma$ in 2D, we report that the value of γ obtained in 2D at $Pe = 0.8 \times 10^4$ is close to 1.2, in agreement with the value $\gamma = 1.208 \pm 0.008$ reported in [14]. Nevertheless, we have found that the value of the scaling exponent γ reduces at increasing Pe, suggesting that it may be affected by finite Pe and/or finite time corrections.

The fact that the mixing layer in 2D grows faster than in 3D has no *a priori* implications on the Nu-Ra scaling since both quantities depend on h . Nonetheless, as shown in Fig. 3(a), dimensionality plays an important role also in the transfer of mass since in 2D the Nusselt number at a given Rayleigh number is much larger than in 3D. For large values of Ra, we observe a linear Nu-Ra relation also in 2D but with a coefficient which is about two times larger than in the three-dimensional case. As discussed above, a larger value of the Nusselt number means a larger correlation between the vertical velocity and the density fluctuations which, in the present case, is a consequence of more elongated and coherent plumes. The scaling regime $Nu \simeq Re$ has been observed also in the case of RB convection in porous media [16,17] but with an opposite dependence of the numerical prefactor on the dimensionality: in RB the coefficient in three dimensions is approximately 40% larger than in two dimensions [16,17], while in RT we find that in two dimensions the coefficient is almost two times larger than in 3D.

In conclusion, we have studied by means of extended direct numerical simulations of the Darcy-Boussinesq equation, the dynamics of Rayleigh-Taylor mixing in three-dimensional porous media in a range of parameters relevant for applications such as CO₂ sequestration in saline aquifers [21]. We have found that the growth of the mixing layer (i.e., plume elongation) follows accurately the dimensional linear prediction with a coefficient which weakly depends on the diffusivity. The horizontal width of density plumes is observed to grow much slower following a diffusive law. The mass-transfer Nusselt number is found to grow linearly with respect to the Rayleigh number, again in agreement with the dimensional prediction, with a coefficient which is independent on the diffusivity (in the limit of large Ra). The comparison of the results with the outcome of two-dimensional simulations at the same diffusivity and resolution shows qualitative similarities but important quantitative differences, therefore suggesting caution in the use of 2D simulations and/or experiments for the modeling of 3D applications such as, for example, the effectiveness of CO₂ sequestration based on the reservoir parameters. Moreover, our results stimulate further studies aimed to investigate the transition between the 3D and the 2D regimes, which is expected to occur in confined geometries at varying the relative extension of the horizontal scales.

We acknowledge support by the Departments of Excellence grant (MIUR) and the computing resources by HPC Center CINECA (IscriB-Pourun grant). We also thank A. Mazzino for useful remarks.

-
- [1] G. Boffetta, A. Mazzino, S. Musacchio, and L. Vozella, Kolmogorov scaling and intermittency in Rayleigh-Taylor turbulence, *Phys. Rev. E* **79**, 065301(R) (2009).
 - [2] M. Chertkov, Phenomenology of Rayleigh-Taylor Turbulence, *Phys. Rev. Lett.* **91**, 115001 (2003).
 - [3] A. Celani, A. Mazzino, and L. Vozella, Rayleigh-Taylor Turbulence in Two Dimensions, *Phys. Rev. Lett.* **96**, 134504 (2006).
 - [4] G. Boffetta, F. De Lillo, and S. Musacchio, Bolgiano scale in confined Rayleigh-Taylor turbulence, *J. Fluid Mech.* **690**, 426 (2012).
 - [5] D. H. Sharp, An overview of Rayleigh-Taylor instability, *Physica D (Amsterdam, Neth.)* **12**, 3 (1984).
 - [6] G. Boffetta and A. Mazzino, Incompressible Rayleigh-Taylor turbulence, *Annu. Rev. Fluid Mech.* **49**, 119 (2017).

- [7] Y. Zhou, Rayleigh–Taylor and Richtmyer-Meshkov instability induced flow, turbulence, and mixing. I, *Phys. Rep.* **720-722**, 1 (2017).
- [8] P. G. Saffman and G. I. Taylor, The penetration of a fluid into a porous medium or Hele-Shaw cell containing a more viscous liquid, *Proc. R. Soc. London, Ser. A* **245**, 312 (1958).
- [9] R. A. Wooding, Growth of fingers at an unstable diffusing interface in a porous medium or Hele-Shaw cell, *J. Fluid Mech.* **39**, 477 (1969).
- [10] H. E. Huppert and J. A. Neufeld, The fluid mechanics of carbon dioxide sequestration, *Annu. Rev. Fluid Mech.* **46**, 255 (2014).
- [11] J. Ennis-King and L. Paterson, Role of convective mixing in the long-term storage of carbon dioxide in deep saline formations, *SPE J, Soc. Pet. Eng. J.* **10**, 349 (2005).
- [12] H. Emami-Meybodi, H. Hassanzadeh, C. P. Green, and J. Ennis-King, Convective dissolution of CO₂ in saline aquifers: Progress in modeling and experiments, *Int. J. Greenhouse Gas Control* **40**, 238 (2015).
- [13] S. S. Gopalakrishnan, J. Carballido-Landeira, A. De Wit, and B. Knaepen, Relative role of convective and diffusive mixing in the miscible Rayleigh-Taylor instability in porous media, *Phys. Rev. Fluids* **2**, 012501 (2017).
- [14] M. De Paoli, F. Zonta, and A. Soldati, Rayleigh-Taylor convective dissolution in confined porous media, *Phys. Rev. Fluids* **4**, 023502 (2019).
- [15] Y. Nakanishi, A. Hyodo, L. Wang, and T. Suekane, Experimental study of 3D Rayleigh-Taylor convection between miscible fluids in a porous medium, *Adv. Water Res.* **97**, 224 (2016).
- [16] D. R. Hewitt, J. A. Neufeld, and J. R. Lister, Ultimate Regime of High Rayleigh Number Convection in a Porous Medium, *Phys. Rev. Lett.* **108**, 224503 (2012).
- [17] D. R. Hewitt, J. A. Neufeld, and J. R. Lister, High Rayleigh number convection in a three-dimensional porous medium, *J. Fluid Mech.* **748**, 879 (2014).
- [18] M. Muskat, *The Flow of Homogeneous Fluids Through Porous Media* (McGraw-Hill, New York, 1937).
- [19] D. A. Nield and A. Bejan, *Convection in Porous Media* (Springer, New York, 2006).
- [20] J. P. Boyd, *Chebyshev and Fourier Spectral Methods* (Dover, New York, 2001).
- [21] S. Backhaus, K. Turitsyn, and R. E. Ecke, Convective Instability and Mass Transport of Diffusion Layers in a Hele-Shaw Geometry, *Phys. Rev. Lett.* **106**, 104501 (2011).
- [22] R. A. Wooding, The stability of an interface between miscible fluids in a porous medium, *J. Appl. Math. Phys. (ZAMP)* **13**, 255 (1962).
- [23] P. M. J. Trevelyan, C. Almarcha, and A. De Wit, Buoyancy-driven instabilities of miscible two-layer stratifications in porous media and Hele-Shaw cells, *J. Fluid Mech.* **670**, 38 (2011).
- [24] A. Celani, A. Mazzino, P. Muratore-Ginanneschi, and L. Vozella, Phase-field model for the Rayleigh–Taylor instability of immiscible fluids, *J. Fluid Mech.* **622**, 115 (2009).
- [25] See Supplemental Material at <http://link.aps.org/supplemental/10.1103/PhysRevFluids.5.062501> for a linear stability analysis of a piecewise-linear profile and the implications on the requirements of numerical simulations.
- [26] G. Boffetta, F. De Lillo, and S. Musacchio, Nonlinear Diffusion Model for Rayleigh-Taylor Mixing, *Phys. Rev. Lett.* **104**, 034505 (2010).
- [27] S. B. Dalziel, P. F. Linden, and D. L. Youngs, Self-similarity and internal structure of turbulence induced by Rayleigh–Taylor instability, *J. Fluid Mech.* **399**, 1 (1999).
- [28] W. H. Cabot and A. W. Cook, Reynolds number effects on Rayleigh–Taylor instability with possible implications for type Ia supernovae, *Nat. Phys.* **2**, 562 (2006).
- [29] C. R. Doering and P. Costantin, Bounds for heat transport in a porous layer, *J. Fluid Mech.* **376**, 263 (1998).
- [30] J. Otero, L. A. Dontcheva, H. Johnston, R. A. Worthing, A. Kurganov, G. Petrova, and C. R. Doering, High-Rayleigh-number convection in a fluid-saturated porous layer, *J. Fluid Mech.* **500**, 263 (2004).